Inorg. Chem. **2004**, *43*, 3292–3298

Electrochemical Investigations of the [Tris(2-(diphenylphosphino)thiaphenolato)ruthenate(II)] Monoanion Reveal Metal- and Ligand-Centered Events: Radical, Reactivity, and Rate

Craig A. Grapperhaus* and Selma Poturovic

Department of Chemistry, University of Louisville, Louisville, Kentucky 40292

Received September 12, 2003

Electrochemical investigations of [bis(triphenylphosphoranylidene)ammonium)][tris(2-(diphenylphosphino)thiaphenolato)-ruthenate(II)], PPN[Ru(DPPBT)$_3$] (**1**), and [(bis(2-(diphenylphosphino)thiaphenolato)methane)(2-(diphenylphosphino)-thiaphenolato)ruthenium(II)] chloride, [Ru((DPPBT)$_2$CH$_2$)(DPPBT)]Cl (**2**) are reported. Complex **1** is oxidized reversibly in a metal-centered event by one electron at a potential of +455 mV (vs Ag/AgCl) to the ruthenium(III) derivative [tris(2-(diphenylphosphino)thiaphenolato)ruthenium(III)], **3**. Complex **3** can also be prepared by iodine oxidation of **1** in acetonitrile. Oxidation of **3** in acetonitrile is reversible on a cyclic voltammetry time scale but irreversible upon bulk oxidation yielding Ru–X. Monitoring the oxidation of **3** by UV–visible spectroscopy reveals a proposed metal-coordinated thiyl radical intermediate with a maximum absorbance at 850 nm. This intermediate decays at a temperature of –20 °C with a rate constant of (5.82 ± 0.73) × 10^{-3} s^{-1} with a small, positive $\Delta H^{\ddagger}$ and a large, negative $\Delta S^{\ddagger}$. Ru–X can be oxidized reversibly to Ru–Y at a potential of +806 mV but cannot be reduced. Complex **2** is reversibly oxidized by one electron in a metal-centered event to **4** at a potential of +767 mV.

Introduction

The sulfur-centered reactivity of transition metal thiolates is well-established including alkylation, oxygenation, and metalation.[1−5] These reactions may be considered as the attack of a nucleophilic sulfur on an electrophilic reagent. This has been confirmed by several theoretical investigations that conclude the highest occupied molecular orbital of many metal thiolates is a sulfur orbital with significant p character.[6−15] Given the significant ligand character of the HOMO in these complexes, the possibility that oxidation may be ligand-based garners consideration. In fact, largely irreversible oxidation events of metal thiolates have been in some cases assigned as ligand-centered with disulfide as the presumed product.[4,16−22] However, several examples of stabilized thiyl radical complexes, which may demonstrate

* Author to whom correspondence should be addressed. E-mail: grapperhaus@louisville.edu. Phone: (502) 852-5932. Fax: (502) 852-8149.

(1) Thompson, M. C.; Busch, D. H. *J. Am. Chem. Soc.* **1964**, *86*, 3651.
(2) Constable, E. C. *Metals and Ligand Reactivity: An Introduction to the Organic Chemistry of Metal Complexes*, 2nd ed.; VCH: Weinheim, Germany, 1996.
(3) Musie, G.; Reibenspies, J. H.; Darensbourg, M. Y. *Inorg. Chem.* **1998**, *37*, 302−310.
(4) Grapperhaus, C. A.; Darensbourg, M. Y. *Acc. Chem. Res.* **1998**, *31*, 451−459.
(5) Darensbourg, M. Y.; Tuntulani, T.; Reibenspies, J. H. *Inorg. Chem.* **1995**, *34*, 6287−6294.
(6) Ashby, M. T.; Enemark, J. H.; Lichtenberger, D. L. *Inorg. Chem.* **1988**, *27*, 191−197.
(7) Ashby, M. T.; Alguindigue, S. S.; Khan, M. A. *Inorg. Chim. Acta* **1998**, *270*, 227−237.
(8) Randall, D. W.; George, S. D.; Hedman, B.; Hodgson, K. O.; Fujisawa, K.; Solomon, E. I. *J. Am. Chem. Soc.* **2000**, *122*, 11620−11631.
(9) McGuire, D. G.; Khan, M. A.; Ashby, M. T. *Inorg. Chem.* **2002**, *41*, 2202−2208.
(10) Chisholm, M. H.; Davidson, E. R.; Pink, M.; Quinian, K. B. *Inorg. Chem.* **2002**, *41*, 3437−3443.
(11) Costuas, K.; Valenzuela, M. L.; Vega, A.; Moreno, Y.; Peña, O.; Spodine, E.; Saillard, J.-Y.; Diaz, C. *Inorg. Chim. Acta* **2002**, *329*, 129−134.
(12) Ghosh, P.; Bill, E.; Weyhermuller, T.; Neese, F.; Wieghardt, K. *J. Am. Chem. Soc.* **2003**, *125*, 1293−1308.
(13) Bellefeuille, J. A.; Grapperhaus, C. A.; Derecskei-Kovacs, A.; Reibenspies, J. H.; Darensbourg, M. Y. *Inorg. Chim. Acta* **2000**, *300*, 73−81.
(14) Kaasjager, V. E.; Bouwman, E.; Gorter, S.; Reedijk, J.; Grapperhaus, C. A.; Reibenspies, J. H.; Smee, J. J.; Darensbourg, M. Y.; Derecskei-Kovacs, A.; Thomson, L. M. *Inorg. Chem.* **2002**, *41*, 1837−1844.
(15) Grapperhaus, C. A.; Li, M.; Patra, A. K.; Poturovic, S.; Kozlowski, P. M.; Zgierski, M. Z.; Mashuta, M. S. *Inorg. Chem.* **2003**, *42*, 4382−4388.
(16) Hsiao, Y. M.; Chojnacki, S. S.; Hinton, P.; Reibenspies, J. H.; Darensbourg, M. Y. *Organometallics* **1993**, *12*, 870−875.
(17) Kumar, M.; Day, R. O.; Colpas, G. J.; Maroney, M. J. *J. Am. Chem. Soc.* **1989**, *111*, 5974−5976.

10.1021/ic035085u CCC: $27.50
Published on Web 04/22/2004

reversible oxidation behavior, have been reported. Wieghardt et al. reported a series of phenylthiyl- radical and related complexes.[12,23−27] Very recently, Liaw and co-workers reported details of a nickel-coordinated thiyl radical, including X-ray absorption spectroscopy.[28] Previously, Darensbourg and co-workers reported EPR spectroscopy and performed Hückel calculations on RS•[Cr(CO)$_5$]$_2$,[29] while Noble et al. generated, trapped, and studied the reactivity of a dimolybdothiyl complex from photolysis.[30] To date, work on alkyl- and phenylthiyl radicals generated from thiolate ligands has largely focused on first-row transition metals. A notable exception is ruthenium.[31]

The chemistry of ruthenium thiolate complexes is well-known. Ruthenium thiolate complexes have been reported in numerous oxidation states including II, III, and IV.[32−39] However, sulfur-centered reactivity of ruthenium thiolates has precedent. Wieghardt and co-workers reported that oxidation of a TACN−trithiolato−ruthenium(III) complex is an overall 4 electron process resulting in a dinuclear ruthenium(II) complex linked by three disulfide bonds.[31] Recently we reported the isolation of the mono-anion [tris(2-(diphenylphosphino)thiaphenolato)ruthenate-(II)],[Ru(DPPBT)$_3$]$^-$ (anion of **1**), as the crystalline PPN salt and its reaction with dichloromethane under ambient conditions to yield an S-alkylated dithioether/thiolate ruthenium-(II) complex (**2**), Scheme 1.[40] The anion of **1** was first reported by Dilworth, as the triethylammonium salt, and shown to undergo reactivity with dioxygen to generate a sulfur−oxygenated complex.[41] Given the inclination of **1** toward S-centered reactivity, we questioned the "redox-innocence" of this ligand. Previous reports of the redox properties of the anion of **1** are complicated by the poor solubility of the triethylammonium salt and its oxygen sensitivity.[41] Therefore, we initiated a full investigation of the redox properties of the anion of **1** as the PPN derivative and its alkylated analogue under anaerobic conditions. In this manuscript, we report electrochemical investigations of these complexes including cyclic voltammetry, spectroelectrochemical coulometry, and chronoamperometry.

Scheme 1

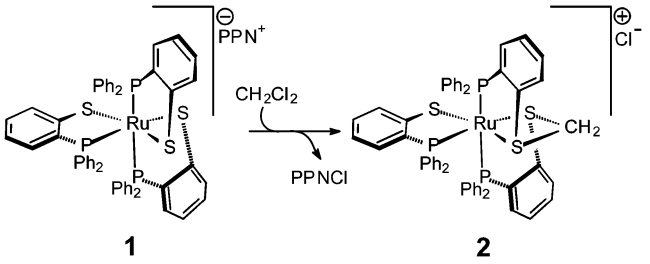

Experimental Section

Materials and Reagents. Methanol and diethyl ether were purified and dried using standard procedures. All the chemical reagents were commercially obtained and used without further purification. Synthesis of PPN[Ru(DPPBT)$_3$] (**1**) and [Ru(DPPBT)$_2$-(DPPBTCH$_2$)]Cl (**2**) has been previously published.[40] All reactions were carried under a nitrogen atmosphere unless otherwise noted.

[Ru(DPPBT)$_3$] (3). To a yellow suspension of **1** (0.258 g, 0.1698 mmol) in methanol (70 mL) was added iodine (0.022 g, 0.085 mmol) with stirring. After 2 h the original yellow solid became red-brown. The solid was filtered onto a fine frit, and it was washed with 2 × 50 mL of methanol and 2 × 50 mL of diethyl ether. The crude product was dissolved in toluene and gravity filtered to remove residual PPNI. Removal of toluene under reduced pressure yielded a fine red brown powder. Yield: 0.120 g (72%). IR (KBr, cm^{-1}): 3049, 1430, 1243, 1093. Electronic absorption spectra [λ_{max}, nm (ϵ)]: 540 (1090), 797 (200), 1041 (3020). Anal. Found (calcd) for $C_{54}H_{42}P_3S_3Ru$: C, 65.85 (66.13); H, 4.11 (4.28).

Physical Methods. IR spectroscopy was obtained using a Thermo Nicolet Avatar 360 spectrometer with a 4 cm^{-1} resolution. X-band EPR spectra were collected on a Bruker EMX EPR spectrometer at 77 K in a Suprasil quartz dewar. An Agilent 8453 diode array spectrometer was used for electronic absorption spectroscopy. Elemental analyses were performed by Midwest Microlab (Indianapolis, IN). Mass spectra were recorded at the University of Louisville Mass Spectrometry Core Laboratory. All electrochemical experiments were performed with an EG&E 273 potentiostat/galvenostat.

Electrochemical and spectroelectrochemical measurements were carried in the 10 mL cell that was designed by E. Bothe of the

(18) Colpas, G. J.; Maroney, M. J.; Bagyinka, C.; Kumar, M.; Willis, W. S.; Suib, S. L.; Baidya, N.; Mascharak, P. K. *Inorg. Chem.* **1991**, *30*, 920−928.
(19) Franolic, J. D.; Wang, W. Y.; Millar, M. *J. Am. Chem. Soc.* **1992**, *114*, 6587−6588.
(20) Millar, M.; Lee, J. F.; O'Sullivan, T.; Koch, S. A.; Fikar, R. *Inorg. Chim. Acta* **1996**, *243*, 333−343.
(21) Hsu, H.-F.; Koch, S. A.; Popescu, C. V.; Münck, E. *J. Am. Chem. Soc.* **1997**, *119*, 8371−8372.
(22) Noveron, J. C.; Herradora, R.; Olmstead, M. M.; Mascharak, P. K. *Inorg. Chim. Acta* **1999**, *285*, 269−276.
(23) Kimura, S.; Bill, E.; Bothe, E.; Weyhermuller, T.; Wieghardt, K. *J. Am. Chem. Soc.* **2001**, *123*, 6025−6039.
(24) Herebian, D.; Bothe, E.; Bill, E.; Weyhermuller, T.; Wieghardt, K. *J. Am. Chem. Soc.* **2001**, *123*, 10012−10023.
(25) Bachler, V.; Olbrich, G.; Neese, F.; Wieghardt, K. *Inorg. Chem.* **2002**, *41*, 4179−4193.
(26) Ghosh, P.; Begum, A.; Herebian, D.; Bothe, E.; Hildenbrand, K.; Weyhermuller, T.; Wieghardt, K. *Angew. Chem., Int. Ed.* **2003**, *42*, 563.
(27) Ray, K.; Weyhermuller, T.; Goossens, A.; Craje, M. W. J.; Wieghardt, K. *Inorg. Chem.* **2003**, *42*, 4082−4087.
(28) Hsieh, C. H.; Hsu, I. J.; Lee, C. M.; Ke, S. C.; Wang, T. Y.; Lee, G. H.; Wang, Y.; Chen, J. M.; Lee, J. F.; Liaw, W. F. *Inorg. Chem.* **2003**, *42*, 3925−3933.
(29) Springs, J.; Janzen, C. P.; Darensbourg, M. Y.; Calabrese, J. C.; Krusic, P. J.; Verpeaux, J. N.; Amatore, C. *J. Am. Chem. Soc.* **1990**, *112*, 5789−5797.
(30) Lizano, A. C.; Munchhof, M. G.; Haub, E. K.; Noble, M. E. *J. Am. Chem. Soc.* **1991**, *113*, 9204−9210.
(31) Albela, B.; Bothe, E.; Brosch, O.; Mochizuki, K.; Weyhermuller, T.; Wieghardt, K. *Inorg. Chem.* **1999**, *38*, 5131−5138.
(32) Koch, S. A.; Millar, M. *J. Am. Chem. Soc.* **1983**, *105*, 3362−3363.
(33) Sellmann, D.; Geck, M.; Knoch, F.; Moll, M. *Inorg. Chim. Acta* **1991**, *186*, 187−198.
(34) Sellmann, D.; Ruf, R.; Knoch, F.; Moll, M. *Inorg. Chem.* **1995**, *34*, 4745−4755.
(35) Zhang, Q.-F.; Lai, C.-Y.; Wong, W.-Y.; Leung, W.-H. *Organometallics* **2002**, *21*, 4017−4020.
(36) Zhang, Q.-F.; Cheung, F. K. M.; Wong, W. Y.; Williams, I. D.; Leung, W.-H. *Organometallics* **2001**, *20*, 3777−3781.
(37) Leung, W. H.; Lau, K. K.; Zhang, Q. F.; Wong, W. T.; Tang, B. Z. *Organometallics* **2000**, *19*, 2084−2089.
(38) Belchem, G.; Steed, J. W.; Tocher, D. A. *J. Chem. Soc., Dalton Trans.* **1994**, 1949−1962.
(39) Belchem, G.; Steed, J. W.; Tocher, D. A. *J. Organomet. Chem.* **1993**, *460*, C30−C33.
(40) Grapperhaus, C. A.; Poturovic, S.; Mashuta, M. S. *Inorg. Chem.* **2002**, *41*, 4309−4311.
(41) Dilworth, J. R.; Zheng, Y. F.; Lu, S. F.; Wu, Q. J. *Transition Met. Chem.* **1992**, *17*, 364−368.

Max-Planck Institute für Bioanorganische Chemie, Mülheim, Germany. The cell is equipped with quartz windows with a 0.5 cm path length. The sample holder and cell were connected in a series to a circulating bath. To prevent condensation of the quartz cell during low-temperature measurements, the cell holder and the cell were placed in custom-built Plexiglas box fitted with Dynasil 4000 quartz windows (Pacific Quartz), through which nitrogen gas was purged. UV−vis and coulometric measurements were taken simultaneously on a 10 mL acetonitrile solution with 0.1 M TBA(PF_6) as a supporting electrolyte. Coulometric measurements were obtained using platinum mesh as a working electrode and platinum mesh as a counter electrode, and Ag^0/Ag^+ was used as a reference electrode. Nitrogen bubbling through the solution was used to prevent oxygen diffusion and for solution mixing. During routine measurements, the circulating bath was set at −34 °C during the coulometry resulting in a measured temperature inside the cell before and after collection of −22 ± 3 °C. After each preformed oxidation, the working electrode was switched to a glassy carbon electrode, bubbling was stopped, and a square wave voltammogram was obtained. After each event, an aliquot was transferred to cooled EPR tube and then frozen for a X-band EPR data analysis.

Chronoamperometry was employed to calculate kinetic parameters.[42] Measurements were obtained using various concentrations in 10 mL of acetonitrile at actual temperature in the cell −20, −10, and −1.5 °C with chiller settings at −34, −16, and −6 °C, respectively. For each temperature, at least four independent measurements of k were performed; see Table S1. In all measurements instrument delay time was set to 0, with an initial potential of +0.620 V, a first potential +0.620 V, t_1 at 150 s, switching potential at 0 V, and a final time, t_2, of 1000 s. During measurements the solution was stirred via argon bubbling. Coulometric charge in the forward direction, Q_f, together with coulometric charge in the back direction, Q_b, was determined from the Q vs t plot. The ratio of Q_b and Q_f was used to determine a first-order rate constant, k. For an EC mechanism the equation used for this calculation is shown as

$$\frac{Q_b}{Q_f} = \frac{p^2}{k^2 - p^2}\left(\frac{1 - e^{(p-k)t_1}}{e^{pt_1} - 1}\right)$$

The p-term represents the mass diffusion coefficient and was calculated from the equation

$$p = -t^{-1} \ln\left(1 - \frac{Q_f}{Q^0_f}\right)$$

Activation parameters $\Delta S^{\ddagger}$ and $\Delta H^{\ddagger}$ were calculated from an Eyring plot. Rate constants used for this plot were average k values at each temperature.

Results

The synthetic protocol for PPN[Ru^{II}(DPPBT)$_3$] (**1**) and [Ru^{II}((DPPBT)$_2CH_2$)(DPPBT)]Cl (**2**) has been previously reported along with structural and spectroscopic characterization.[40] The neutral, trithiolato complex, [Ru^{III}(DPPBT)$_3$] (**3**), is prepared by iodine oxidation of **1** in methanol. Extraction with toluene separates **3** from PPNI yielding an analytically pure red-brown solid following removal of solvent. The infrared spectrum of **3** displays characteristic bands at 3049, 1098, and 530 cm^{-1}, which is similar to that of **1** with the absence of some nonoverlapping peaks associated with the PPN counterion. The UV−vis spectrum of **3** recorded in acetonitrile exhibits maxima at 540 (1090), 797 (200), and 1041 (3020) nm with higher energy bands at 399 and 359 nm. Complex **3** displays a rhombic EPR signal with g = 2.12, 2.06, and 2.04, Figure S1, consistent with a Ru(III), S = 1/2 system.

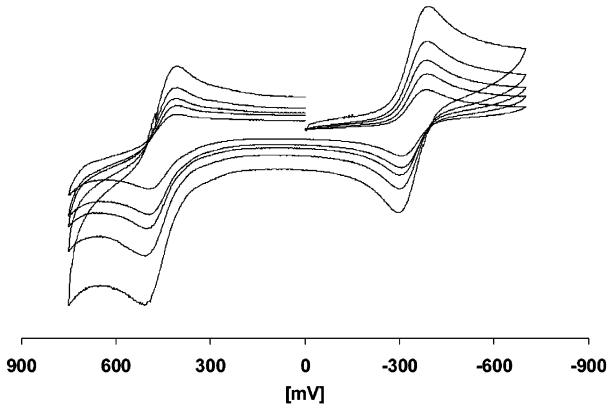

Figure 1. Cyclic voltammogram of **1** in MeCN (1 mM) with 0.1 M (TBA)-PF_6 at scan rates 100, 200, 300, 500, and 1000 mV/s.

Table 1. Summary of Electrochemical Data for **1**, **2**, **3**, and Ru−X

complex	E_{ox},[a] V	E_{red}, V
1	+0.455[b]	−0.345
	+1.13[irr]	
3	+0.455[b]	−0.345
2	+0.767[c]	
Ru−X, Ru−Y	+0.806[d]	

[a] All potentials were obtained at 200 mV/s using a glassy carbon electrode referenced vs Ag/AgCl. [b] Obtained as 1 mM solution in MeCN. [c] 1 mM solution in $MeCl_2$. [d] Obtained during electrolysis as 0. 5mM solution in MeCN.

Figure 1 displays the cyclic voltammogram **1** in acetonitrile at various scan rates. The voltammogram of **1** displays redox couples at −345 and +455 mV at a scan rate of 200 mV/s versus Ag/AgCl, Table 1. An additional irreversible oxidation at +1.13 V, not shown, is assigned to oxidation of the PPN counterion. The CV of **3** is identical, as required, with that of **1** expect for the PPN centered event. The −345 mV couple is independent of scan rate over the range of 100−1000 mV/s with a consistent ΔE of 78−94 mV and is assigned as reversible. The +455 mV couple is also scan rate independent over a range of 100−1000 mV/s.

Bulk oxidation of **1** by controlled potential coulometry, +100 mV, was performed in acetonitrile at −20 °C in a spectroelectrochemical cell (see Experimental Section) equipped with a quartz window to allow collection of UV−visible spectra during oxidation. Spectra were recorded every 0.10 electron equiv during which time the color of the solution changes from yellow to red-brown. A trace of the UV−visible spectra is shown in Figure 2. Following oxidation of **1** by 0.95 electron equiv, the current is negligible indicating a one-electron process. A plot of current versus time displays a typical exponential decay. During oxidation, the absorbance band at 435 nm decreases in intensity while new bands associated with **3** at 540, 797, and 1041 nm increase. An isosbestic point is observed at 477 nm consistent

(42) Bard, A. J.; Tatwawadi, S. V. *J. Phys. Chem.* **1964**, *68*, 2676−2682.

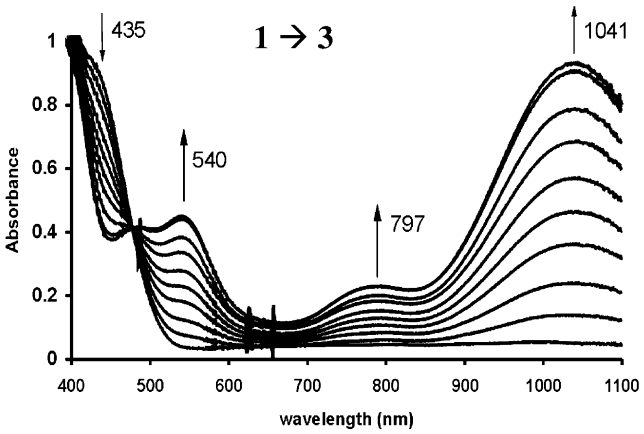

Figure 2. Electronic spectra acquired during oxidation of **1** to **3**. Spectra were obtained every 0.1 electron equiv in MeCN solution at −20 °C.

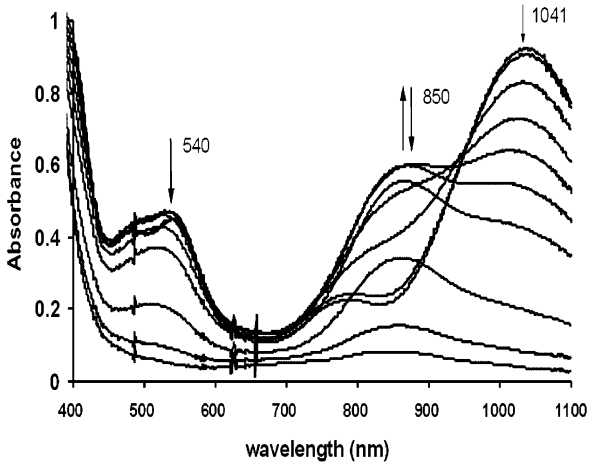

Figure 3. Electronic spectra changes during oxidation of **3** to Ru−X. Spectra were obtained every 0.1 electron equiv in MeCN solution at −20 °C.

with the clean oxidation of **1** to **3**. The EPR spectrum following oxidation is identical with that of genuine **3**. The square-wave voltammogram following oxidation is indistinguishable from that of the initial solution of **1**. The oxidized product, **3**, can be rereduced to **1** by applying the appropriate negative potential. Several cycles of oxidation/reduction do not result in significant changes in the UV−visible trace or voltammogram.

Bulk oxidation of **3** was performed at a potential of +620 mV at −20 °C. Again, UV−visible spectra were recorded every 0.10 electron equiv, Figure 3. The spectra display a steady decrease in the intensity of the 1041 band. An intermediate with intensity at 850 nm grows in but diminishes as the oxidation proceeds and is nearly absent following a complete oxidation (0.95 equiv) of **3**. A plot of current versus time decays exponentially and approaches zero. The oxidation product, Ru−X, is bright yellow. No isobestic points are observed, and the process is irreversible on the electrolysis time scale. Repeated attempts to obtain Ru−X as a solid free of supporting electrolyte were unsuccessful. Addition of chemical oxidants to **3**, such as ceric ammonium nitrate, yield products with spectroscopic features distinct from Ru−X. At room temperature, solutions of Ru−X and supporting electrolyte slowly change from yellow to brown-

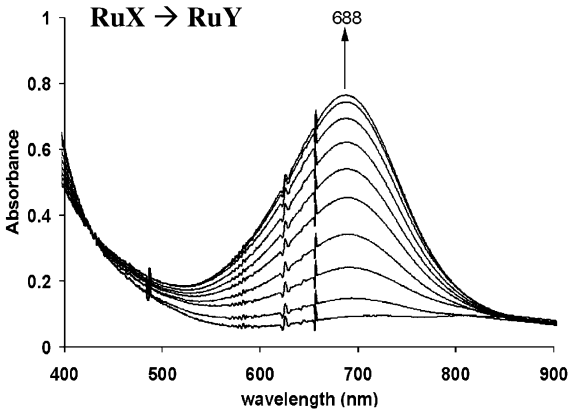

Figure 4. Electronic spectra acquired during oxidation of Ru−X to Ru−Y. Spectra were obtained every 0.1 electron equiv in MeCN solution at −20 °C.

Scheme 2

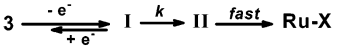

orange. The mass spectrum of the crude reaction mixture of freshly prepared Ru−X is shown in Figure S3. The parent peak at $m/z = 981.1$ displays an isotopic envelope consistent with the mononuclear ruthenium monocation with three DPPBT like ligands (vide infra), Figure S2. The mass spectrum of thermally degraded Ru−X reveal significant peaks assigned to PPN, from **1**, and tetrabutylammonium, from the supporting electrolyte, but no unambiguously assignable peaks from degraded Ru−X. Repeated attempts to isolate the milligram quantities of Ru−X from supporting electrolyte have been unsuccessful.

The square-wave voltammogram of Ru−X, Figure S3, is distinct from that of **1**/**3** and displays a single redox event. Notably, Ru−X cannot be reduced even at negative potentials but rather displays an accessible oxidation at +806 mV. The concentration in the electrochemical cell (0.5 mM) precludes cyclic voltammetric analysis, but the square-wave voltammogram suggests the process is quasi-reversible ($i_{pa}/i_{pc} = 3.3$). Bulk oxidation of Ru−X to Ru−Y was performed at +1.0 V at −20 °C and monitored by UV−vis. Figure 4 displays the trace with data collected every 0.10 electron equiv. During oxidation, a new band at 688 nm increases in intensity and reaches a maximum after full oxidation (0.95 equiv). Additionally, the band at 366 nm shifts to 330 nm. The square-wave voltammogram of Ru−Y is identical with that of Ru−X. Repeated cycles of oxidation (+1.0 V) and reduction (0.00 V) between Ru−X and Ru−Y reproduce the UV−visible trace (and its converse) with no significant changes. An aliquot of Ru−Y was removed via syringe and frozen in an EPR tube. The EPR spectrum of Ru−Y, Figure S4, displays a rhombic signal with $g = 2.09$, 2.05, and 2.03.

The rate of conversion from **3** to Ru−X was monitored by chronoamperometry at three temperatures. Complex **3** was partially oxidized, ∼40% of the bulk, and then rereduced back to **3**. Only a portion of the oxidized product can be rereduced consistent with the chemical reaction of an intermediate, **I**, as shown in Scheme 2. From the ratio of the charge consumed during oxidation and reduction, Q_b/Q_f, a pseudo-first-order rate constant for the chemical step

Table 2. Average k_{obs} for **1** Obtained from Chronoamperometry

T, K	10^3p, s^{-1}	Q_b/Q_f[a]	10^3k, s^{-1}
253	2.64	0.191	5.82 ± 0.73
263	2.32	0.143	7.33 ± 1.49
272	2.84	0.105	10.08 ± 0.56

[a] Determined from oxidation potential at 0.620 V for 150 s and reduction potential at 0 V for 1000 s.

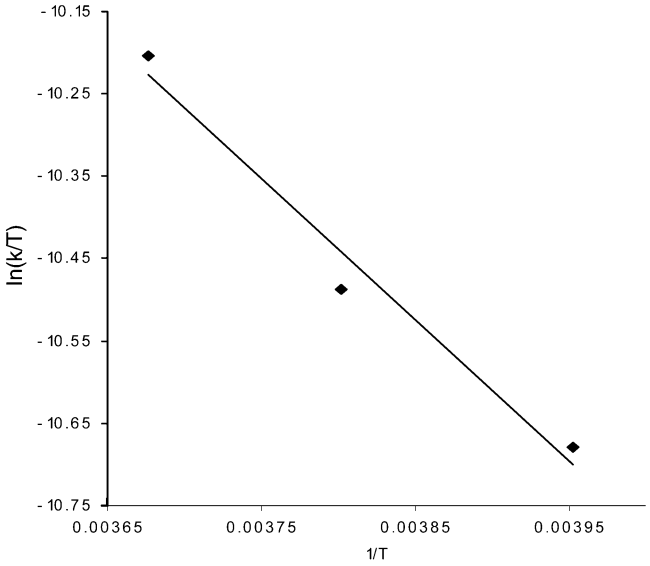

Figure 5. Eyring plot of average k's obtained from chronoamperometery at −20, −10, and −1 °C.

following the oxidation of **3**, i.e. Ru−X formation, can be determined using eq 1.[42] The value p, which can be regarded as an "electrochemical rate constant", is calculated from the current decay curve during oxidation. Values of average p and average Q_b/Q_f for the oxidation of **3** to Ru−X at three temperatures are listed in Table 2 along with average values of k. Individual p and Q_b/Q_f values and associated k values used to calculate the averages are provided in Table S1. Notably, k is independent of the initial concentration of **3** precluding a termination step involving coupling of two intermediates, **I**. From an Eyring plot using average k values at three temperatures, activation parameters can be extracted, Figure 5. The experimental values of $\Delta H^{\ddagger}$ and $\Delta S^{\ddagger}$ are 14 ± 2 kJ/mol and −160 ± 40 J/(mol K), respectively.

$$\frac{Q_b}{Q_t} = \frac{p^2}{k^2 - p^2}\left(\frac{1 - \exp[(p-k)t_1]}{\exp(pt_1) - 1}\right) \qquad (1)$$

The cyclic voltammogram of the S-alkylated complex, **2**, displays a single redox event at +767 mV versus Ag/AgCl in acetonitrile, Table 1. The $E_{1/2}$ and ΔE values are constant over a scan rate range of 100 to 1000 mV/s. Bulk oxidation of **2** was performed at +1.1 V at −20 °C with monitoring by UV−visible spectroscopy, Figure S5. Oxidation proceeds as a one-electron process yielding $[Ru^{III}((DPPBT)_2CH_2)(DPPBT)]^{2+}$ (**4**). During oxidation a new band at 672 nm grows in intensity. The square-wave voltammogram of the oxidized product, **4**, is identical with that of **2**. The process is reversible on the coulometry time scale, and several cycles of oxidation and reduction do not result in significant spectroscopic or voltammetric changes. Following oxidation, an aliquot of **4** was removed and frozen for EPR analysis. The EPR spectrum, Figure S6, shows a rhombic signal with $g = 2.12$, 2.06, and 2.04. Complex **4** may also be prepared by chemical oxidation of **2** with reagents such as ceric ammonium nitrate.

Discussion

The oxidation of metal thiolate complexes is complicated by the potential noninnocence of thiolate donors. In this regard, assignment of redox events as metal-based or ligand-based is difficult and often tentatively made on the basis of the reversibility of the redox couple in the cyclic voltammogram. Recently, Wieghardt et al. and others have reported a growing number of stabilized thiyl radicals thus greatly enhancing knowledge in this field.[12,23−30,43−49] As many of these examples involve amino−thiophenol chelates, we decided to investigate the electrochemical oxidation of the phosphine−thiophenol ruthenium complexes we had been previously investigating due to their rich S-centered reactivity.

The first oxidation of **1** is a reversible, metal-centered oxidation of Ru(II) (**1**) to Ru(III) (**3**). The process is reversible on both the CV and coulometry time scale, and the product's identity is confirmed by independent synthesis. The second oxidation, from **3** to Ru−X, is complex. The oxidation is reversible on the CV time scale but irreversible on the coulometry time scale indicating a stabilized intermediate. This intermediate is observable during controlled-potential oxidation as a species with a λ_{max} of 850 nm. The intermediate decays prior to a full one-electron oxidation. The intermediate may contain either a transiently stable Ru(IV) thiolate or a Ru(III) thiyl radical. The cobalt phenylthiyl derivative of TACN reported by Wieghardt displays absorption maxima at 509 and 784 nm (with a shoulder at 670 nm).[23] Additionally, both the Au(III) *o*-dithiobenzosemiquinonate radical complex reported by Wieghardt and the oxidized nickel *o*-dithiobenzosemiquinonate complex of Sellmann display intense intervalence bands at 1452 and 860 nm, respectively, although the corresponding Co(III) derivative lacked such a band > 700 nm.[27,50] Notably, the molar absorptivities of these bands are 2.6×10^3 and 1.03×10^3. A minimum ϵ for our intermediate (assuming the concentration of the thiyl radical after 0.5 equiv oxidation equals half the initial concentration of **3**) is 4.8×10^3. Thus,

(43) Sawyer, D. T.; Srivatsa, G. S.; Bodini, M. E.; Schaefer, W. P.; Wing, R. M. *J. Am. Chem. Soc.* **1986**, *108*, 936−942.
(44) Kumar, M.; Day, R. O.; Colpas, G. J.; Maroney, M. J. *J. Am. Chem. Soc.* **1989**, *111*, 5974−5976.
(45) Deters, D.; Hartmann, H. J.; Weser, U. *Biochim. Biophys. Acta* **1994**, *1208*, 344−347.
(46) Green, M. T. *J. Am. Chem. Soc.* **1999**, *121*, 7939−7940.
(47) Lim, B. S.; Fomitchev, D. V.; Holm, R. H. *Inorg. Chem.* **2001**, *40*, 4257−4262.
(48) Branscombe, N. D. J.; Atkins, A. J.; Marin-Becerra, A.; McInnes, E. J. L.; Mabbs, F. E.; McMaster, J.; Schroder, M. *J. Chem. Soc., Chem. Commun.* **2003**, 1098−1099.
(49) Sellmann, D.; Geck, M.; Knoch, F.; Ritter, G.; Dengler, J. *J. Am. Chem. Soc.* **1991**, *113*, 3819−3828.
(50) Sellmann, D.; Binder, H.; Haussinger, D.; Heinemann, F. W.; Sutter, J. *Inorg. Chim. Acta* **2000**, *300*, 829−836.

the spectroscopic evidence is most consistent with a metal-coordinated thiyl radical intermediate and is assigned as such.

The metal-coordinated thiyl radical generated upon oxidation of **3** slowly rearranges in a chemical step to Ru−X. First-order rate constants for this step were determined at three temperatures, Table 2, with $k_{obs} = (5.82 \pm 0.73) \times 10^{-3}$ s^{-1} at −20 °C. Reliable measurements at higher temperatures were precluded due to significant loss of solvent during oxidation. Rates were measured at a high (∼1 or 3 mM) and low (∼0.5 mM) concentration for each temperature with the limits set by the sensitivity of the detector and solubility of **3** in acetonitrile. The variance in rate constants at a given temperature is random and does not support a bimolecular reaction for which detectable increases in k_{obs} are expected. For example, at −10 °C, the average rate constant at 0.44 ± 0.4 mM is $(8.1 \pm 0.1) \times 10^{-3}$ s^{-1} whereas at 3.0 ± 0.1 mM it is $(6.1 \pm 1.0) \times 10^{-3}$ s^{-1}. If the reaction were second order in **3**, the observed first-order rate constant at 3 mM should be significantly higher.

The activation parameters determined from the plot in Figure 5 reveal a small, positive enthalpy of activation and a large, negative entropy of activation. Although the absolute values of these parameters are difficult to assign given the error in individual measurements of *k* and the small temperature range, we contend their magnitude and sign are correct. Although, a large negative entropy suggests an intermolecular process, the independence of *k* as a function of the concentration of **3** and electrochemical measurements of Ru−X (vide infra) make a binuclear route unlikely. Alternatively, the solvent, acetonitrile may play a significant role. This may be expected given the reaction between **1** with dichloromethane.[40] However, Ru−X is also generated when **3** is oxidized in dimethylformamide precluding a role for solvent in the final product.

Ru−X, and its oxidized derivative Ru−Y, has been characterized in solution by UV−visible spectroscopy, cyclic voltammetry and coulometry, EPR, and mass spectroscopy. The mass spectrum of freshly prepared Ru−X is consistent with 3 DPPBT ligands and a single Ru, Figure S2. While this is consistent with a mononuclear disulfide product, the isotopic envelope is also consistent with the trithiolato precursor, **3**. It is not, however, consistent with a doubly charged binuclear species. Neither Ru−X nor Ru−Y has been isolated as a solid. Ru−X is oxidized by 1 electron/Ru center to Ru−Y at +806 mV. If Ru−X is a binuclear disulfide, analogous to that observed by Wieghardt,[31] this observation would require that oxidation of one metal center does not influence the oxidation potential of the second ruthenium. This is unlikely. Additionally, Ru−Y is EPR active with *g*-values consistent with a mononuclear Ru(III), Table 3.

On the basis of the spectroscopic, electrochemical, and mass spectroscopy data, we tentatively assign Ru−X and Ru−Y as mononuclear, disulfide-coordinated Ru(II) and Ru(III) analogues of **1**. We propose, on the basis of experimental observations and by analogy to the pathway suggested by Wieghardt, the following route for oxidation of **1**, Scheme 3.[31] Following a reversible metal centered

Table 3. Comparison of the Known Complexes **2**/**4** and the Proposed Complexes Ru−X/Ru−Y

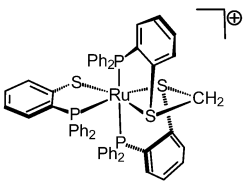	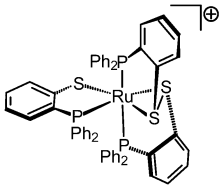
known structure	tentative structure
Ru(II) Mono-cation	Ru(II) Mono-cation
3 phosphine	3 phosphine
1 thiolate	1 thiolate
2 thioether	2 disulfide
4-member ring	3-member ring
$Ru^{III/II}$ = +767 mV	$Ru^{III/II}$ = +806 mV
No reduction	No reduction
Ru^{III} g= 2.12, 2.06, 2.04	Ru^{III} g=2.09, 2.05, 2.03
Ru^{III} λ_{max}=671	Ru^{III} λ_{max}=688

Scheme 3

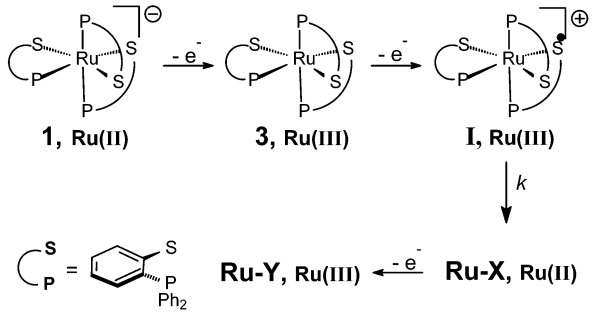

oxidation of **1** to **3**, a ligand-centered oxidation occurs yielding a ruthenium coordinated thiyl radical. This radical has a limited lifetime, making the process reversible/quasi-reversible on the CV time scale but irreversible upon bulk oxidation. From chronoamperometry we determined a rate on the order of 10^{-3} for this process with a small positive $\Delta H^{\ddagger}$ and a large negative $\Delta S^{\ddagger}$. The activation parameters are consistent with a binuclear reaction. However, the observed rate data are inconsistent with a binuclear reaction between two ruthenium complexes. While solvent, or counterion, may be involved, the observed product does not change as these are varied. As an alternative, we suggest formation of an *intramolecular* Ru(III) disulfide radical as the rate-limiting step, which would not require a significant enthalpic barrier, but would require formation of a three member Ru−S−S ring that may be entropically prohibitive, although this is speculative at this time. The proposed product is similar to the *intermolecular* disulfide radical proposed by Wieghardt et al. in a related system.[31] The disulfide radical could then reduce the Ru(III) to Ru(II) in a fast step to yield Ru−X. Ru−X can be further oxidized by 1 electron to Ru−Y. The proposed structure of Ru−X, see Table 3, is similar to the alkylated product, **2**. Similarities of Ru−X and **2** and their oxidized derivatives are highlighted in Table 3.

The generation of the thiyl-radical intermediate and its slow decay brings up several interesting points regarding oxidation of metal thiolate complexes. First, if the metal-coordinated thiyl radical is stabilized, can it react with other

substances in solution as shown with other sulfur centered ligand radicals?[30] We are currently investigating this possibility.[51] Second, if Ru−X is indeed an intramolecular disulfide as tentatively assigned, then this reaction is analogous to the well-known "induced internal electron transfer reactions" first described by Taube and successfully employed synthetically by Stiefel and co-workers in which coordinated sulfides are oxidized to disulfides with metal reduction.[52,53] How general this reaction is for other metal thiolates remains to be determined.

Acknowledgment. We thank E. Bothe (Max Planck Institute für Bioanorganische Chemie, Mülheim, Germany) for the spectroelectrochemical cell design. The insight of K. Wieghardt (MPI für Bioanorganische Chemie) is greatly appreciated. Acknowledgment is made to the donors of the Petroleum Research Fund, administered by the American Chemical Society, for partial support of this research (ACS PRF#37663-G3).

Supporting Information Available: Partial funding also provided by the National Science Foundation (CHE-0238137). X-band EPR spectra of **3** (Figure S1), Ru−Y (Figure S4), and **4** (Figure S6), the mass spectrum of Ru−X (Figure S2), a square wave voltammogram of Ru−X (Figure S3), a UV−visible trace of the oxidation of **2** to **4** (Figure S5), and kinetic data (Table S1) in PDF format. This material is available free of charge via the Internet at http://pubs.acs.org.

IC035085U

(51) Grapperhaus, C. A.; Poturovic, S. Unpublished results.
(52) McConnachie, C. A.; Stiefel, E. I. *Inorg. Chem.* **1999**, *38*, 964−972.
(53) Taube, H. *Electron Transfer Reactions of Complex Ions in Solution*; Academic Press: New York, 1970.